

Mean-Field Predictions of Scaling Prefactors Match Low-Dimensional Jammed Packings

James D. Sartor*, Sean A. Ridout†, Eric I. Corwin*

**Department of Physics and Materials Science Institute,
University of Oregon, Eugene, Oregon 97403, USA*

†*Department of Physics and Astronomy University of Pennsylvania, Philadelphia, Pennsylvania 19104, USA*

(Dated: January 22, 2021)

No known analytic framework precisely explains all the phenomena observed in jamming. The replica theory for glasses and jamming is a mean-field theory which attempts to do so by working in the limit of infinite dimensions, such that correlations between neighbors are negligible. As such, results from this mean-field theory are not guaranteed to be observed in finite dimensions. However, many results in mean field for jamming have been shown to be exact or nearly exact in low dimensions. This suggests that the infinite dimensional limit is not necessary to obtain these results. In this Letter, we perform precision measurements of jamming scaling relationships between pressure, excess packing fraction, and number of excess contacts from dimensions 2–10 in order to extract the prefactors to these scalings. While these prefactors should be highly sensitive to finite dimensional corrections, we find the mean-field predictions for these prefactors to be exact in low dimensions. Thus the mean-field approximation is not necessary for deriving these prefactors. We present an exact, first-principles derivation for one, leaving the other as an open question. Our results suggest that mean-field theories of critical phenomena may compute more for $d \geq d_u$ than has been previously appreciated.

Introduction – Granular materials exhibit universal properties regardless of the material properties of the individual grains [1–3]. The jamming transition is a critical point near which properties such as pressure, packing fraction, or number of excess contacts, among others, scale as power laws. Scaling theory summarizes and condenses these power law relationships, but no first-principles theory of jammed systems at finite dimensions exists. The replica mean-field theory of glasses and jamming has been shown to be exact in the infinite dimensional limit [4, 5]. To do so it relies on the assumption that there are no correlations between neighbors, fundamentally at odds with low-dimensional systems. As such, mean-field predictions should not be expected to hold in low dimensional-jamming, and some results, most notably the packing fraction at jamming, deviate from the mean-field predictions [2, 6]. However, despite the fact that low dimensional systems have highly correlated neighbors the scaling relations are precisely the same as those found in infinite dimensions [7–9]. Many other results predicted by the mean field have also been observed in low dimensional jamming, suggesting that they may be provable without the mean field approximation [2, 3, 10–13].

Here, we move one step further in the comparison between low-dimensional jamming and mean-field jamming by probing not only scaling relations but also prefactors between a handful of properties: pressure P , excess contacts δz , and excess packing fraction above jamming $\Delta\varphi$. We demonstrate the continued success of the mean field in describing low-dimensional systems by quantitatively verifying the mean-field predictions for these prefactors. Thus, the mean-field approximation is overzealous: one need not have vanishing correlations in order to obtain

these results. In this spirit we provide a first-principles proof of the relation between pressure and excess packing fraction free of the mean-field assumptions. These results call out for proofs for all of the other universal relations of the jamming transition.

Background – Granular materials undergo a jamming transition at a critical packing fraction φ_j . The number of force bearing contacts between grains jumps abruptly from zero to the minimum number sufficient to support global rigidity and thus global pressure, Z_c . In a packing of N frictionless, spherical particles in d dimensions, $Z_c = Nd + 1 - d$ [1, 14].

We limit our study to spherical particles interacting through a harmonic contact potential given by

$$U_{ij} = \varepsilon \left(1 - \frac{|\mathbf{r}_{ij}|}{\sigma_{ij}}\right)^2 \Theta \left(1 - \frac{|\mathbf{r}_{ij}|}{\sigma_{ij}}\right), \quad (1)$$

where ε is the energy scale, \mathbf{r}_{ij} is the contact vector between particles i and j , σ_{ij} is the sum of the radii of particles i and j , and Θ is the Heaviside step function. Thus, the total energy $U = \frac{1}{2} \sum_{ij} U_{ij}$. From this potential, the forces between particles can be calculated as

$$\mathbf{f}_{ij} = \frac{2\varepsilon}{\sigma_{ij}} \left(1 - \frac{|\mathbf{r}_{ij}|}{\sigma_{ij}}\right) \Theta \left(1 - \frac{|\mathbf{r}_{ij}|}{\sigma_{ij}}\right) \hat{r}_{ij}. \quad (2)$$

We compute a unit and dimension independent pressure using the microscopic formula [7, 15]

$$P \equiv -\frac{\bar{V}_p}{\varepsilon} \frac{dU}{dV} = \frac{\bar{V}_p}{\varepsilon V d} \sum_{i,j} \mathbf{f}_{ij} \cdot \mathbf{r}_{ij}, \quad (3)$$

where V is the volume of the system and \bar{V}_p is the average particle volume.

For soft spheres the packing fraction φ can be increased, leading to new contacts and an increased pressure. We thus consider three natural quantities that measure distance from jamming:

- excess packing fraction, $\Delta\varphi = \varphi - \varphi_j$
- excess contacts per particle, $\delta z = (Z - Z_c)/N$ where Z is the number of contacts
- pressure P

The relationships between these quantities are predicted by mean-field theory as [5]:

$$P = C_{p\varphi} \Delta\varphi \quad (4)$$

$$\delta z = C_{zp} P^{1/2} \quad (5)$$

with prefactors $C_{p\varphi}$ and C_{zp} which are functions only of spatial dimension [7]. These and other scaling relationships have been previously explained by approximate theories [16–19] and computationally confirmed in low-dimensional jamming [1, 7, 8, 14]. They are summarized concisely by the scaling theory of the jamming transition [9]. The scaling exponents in $d \geq 2$ match those in mean field, suggesting that the transition behaves like a critical point with upper critical dimension $d_u = 2$. Moreover, mean-field theory predictions of these prefactors can be derived as [5, 20]:

$$C_{p\varphi} = \frac{1}{d} \hat{C}_{p\varphi} \quad (6)$$

$$C_{zp} = \frac{d}{\sqrt{2^d}} \hat{C}_{zp} \quad (7)$$

where $\hat{C}_{p\varphi}$ and \hat{C}_{zp} are finite constants in the $d \rightarrow \infty$ limit, which have not yet been explicitly calculated. Note that these relations are presented in a particular choice of units in the literature. We include details of the conversion to our dimensionless units in the Supplemental Material. *A priori*, it is not expected that these predictions will apply in low dimensions, in which the mean-field assumption is not warranted. Even above upper critical dimensions, mean-field theories are not generally expected to correctly compute prefactors, or even the purportedly universal amplitude ratios. Beyond scaling exponents, to our knowledge, the critical cluster shape in percolation and related phenomena [21, 22] and the Binder cumulant in the Ising model [23–25] are the only quantities which are known to be equal to their mean-field values above the upper critical dimension. Even though these prefactors for jamming scaling relationships have been measured and reported [7, 26], because they are not expected to be equal to their mean-field values they have not received substantial theoretical attention. An approximate calculation of the related prefactor between the shear modulus and number of excess contacts has been performed in three dimensions [18].

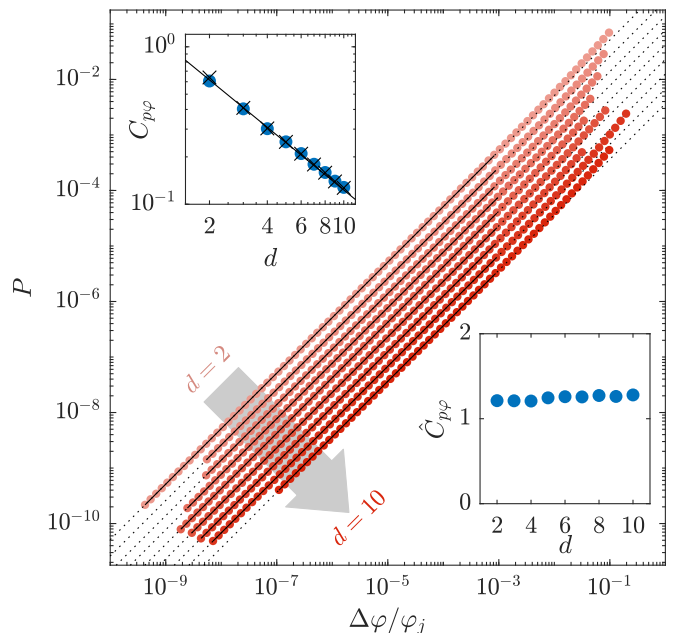


Figure 1. Measured pressure scales linearly with scaled excess packing fraction for systems from $d = 2$ to $d = 10$. Measured values for φ_j in our protocol are included in the Supplemental Material. Black lines show fits for $C_{p\varphi}$ using Eq. 4. We exclude from the fit data with $\Delta\varphi/\varphi_j > 10^{-3}$, to avoid the effect of larger overlaps causing deviations from this power law. Dotted lines show the extension of fits beyond fitted range. Upper inset shows the measured values of $C_{p\varphi}$ (blue circles) to scale in agreement with the mean-field prediction Eq. 6, shown as a fit to a black line with $\hat{C}_{p\varphi} \approx 1.23$. Moreover, they are in precise agreement with predicted values from Eq. 14 (marked with black \times 's). Lower inset shows measured values of $\hat{C}_{p\varphi}$ calculated from the measured values of $C_{p\varphi}$ and eqn 6. While each prefactor is measured from a single system, the prefactors for a second, identically constructed dataset were calculated to be well within the bounds of the marker size.

Computational methods – We use pyCudaPacking [2], a GPU-based simulation engine, to generate energy minimized soft (or penetrable) sphere packings. We do so for number of particles $N = 8192 - 32768$ and dimension $d = 2 - 10$. Our results suggest that $N = 8192$ is large enough to avoid finite size effects in $d < 9$, which we have verified in $d = 8$ by comparing our packing at $N = 8192$ with one at $N = 16384$, finding no deviation. For $d = 9$ and $d = 10$ we use system sizes of 16384 and 32768, respectively. The particles are monodisperse, except in two dimensions in which we use equal numbers of bidisperse particles with a size ratio of 1:1.4 to prevent crystallization.

The packings are subject to periodic boundary conditions. We minimize the packings using the FIRE minimization algorithm [27] using quad precision floating point numbers in order to achieve resolution on the contact network near the jamming point.

Using the same methods as described in Ref. [28],

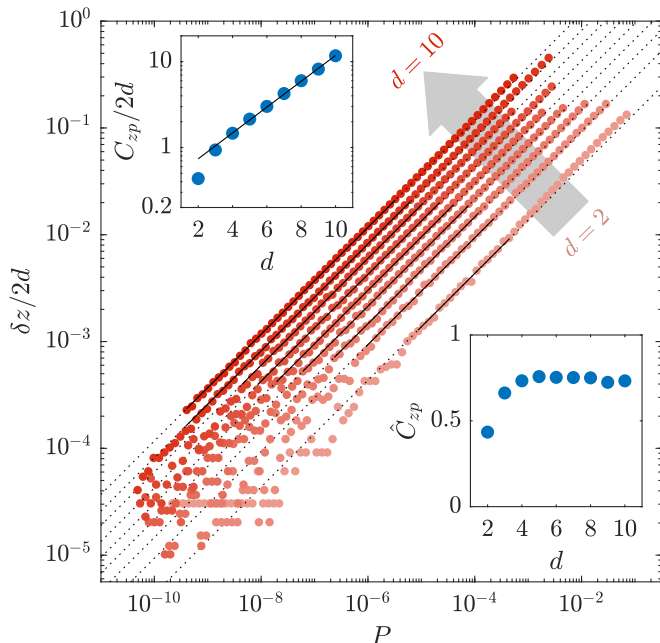


Figure 2. Measured excess contacts scales with the square root of pressure for systems from $d = 2$ to $d = 10$. Black lines show fits for C_{zp} using Eq. 5. For our fits, we ignore high pressure data as in Fig. 1, and additionally exclude data with less than 40 excess contacts to avoid fitting to small number fluctuations. Dotted lines show the extension of our fits beyond fitted range. Lower inset shows the measured values of C_{zp} (blue circles), which scale in agreement with the mean-field prediction Eq. 7, shown as a fit to a black line and with $\hat{C}_{zp} \approx 0.74$. Upper inset shows measured values of \hat{C}_{zp} calculated from the measured values of C_{zp} and Eq. 7. While each prefactor is measured from a single system, the prefactors for a second, identically constructed dataset were calculated to be well within the bounds of the marker size.

we start with randomly distributed initial positions, and apply a search algorithm to create systems approximately logarithmically spaced in $\Delta\varphi$. At each step we use the known power law relationship between energy and $\Delta\varphi$ to calculate an estimate of φ_j . We use this estimate to approximate $\Delta\varphi$ and determine the next value of φ in an effort to logarithmically space $\Delta\varphi$ values. We then adjust the packing fraction to this value of φ by uniformly scaling particle radii and minimizing the system. We continue this process until the system is nearly critically jammed, i.e. has exactly one state of self stress. We then use the known power law relationship between pressure and $\Delta\varphi$ to fit the dataset and precisely calculate φ_j (with error less than the smallest value of $\Delta\varphi$) from which we calculate $\Delta\varphi$ at each value of φ .

Results – Figure 1 shows the measured linear scaling of pressure with packing fraction separately for each dimension. We fit the data to Eq. 4 to find $C_{p\varphi}$, considering only data close to jamming to avoid fitting to high pressure deviations from the scaling power law. The measured values of $C_{p\varphi}$ are shown in the inset to confirm the

$1/d$ dimensional scaling predicted by mean-field theory in Eq. 6. A fit to this scaling provides a value of $\hat{C}_{p\varphi}$ of 1.23.

Figure 2 shows the measured square root scaling of excess contacts with pressure separately for each dimension. We fit the data to Eq. 5 to find C_{zp} , the values of which are shown in the inset. Beginning around three dimensions, the values of C_{zp} confirm the dimensional scaling predicted by mean-field theory in Eq. 7, and a fit to this scaling provides a value of \hat{C}_{zp} of 0.74.

The values of both $C_{p\varphi}$ and C_{zp} are roughly consistent with values measured in previous studies [7, 26]. It has been recently suggested that the prestress, i.e., the normalized ratio of the first and second derivatives of the potential as defined in Ref. [29], is a better candidate to dedimensionalize the relationship between pressure and excess contacts. However, we find a substantially better collapse of our expected form of pressure than with prestress. For more details on prestress, see the attached Supplemental Material.

Discussion – The close agreement of our data with the mean-field predictions in low dimensions suggests that the mean-field assumption is not essential to derive these scaling and prefactor relations. In the spirit of discovering proofs for these relations free of the mean-field assumption, we expand on an earlier calculation of the bulk modulus scaling [17] to show that such a calculation can also explain the scaling of $C_{p\varphi}$ with spatial dimension and the precise value of $\hat{C}_{p\varphi}$.

From taking a derivative of Eq. 4, we see immediately that $C_{p\varphi}$ may be expressed in terms of the bulk modulus, $K \equiv V \frac{d^2 U}{dV^2}$, at jamming:

$$C_{p\varphi} = \frac{\bar{V}_p V}{\varphi \varepsilon} \frac{d^2 U}{dV^2} = \frac{V}{N \varepsilon} K. \quad (8)$$

We note that this approximation slightly overestimates $C_{p\varphi}$: the apparently linear average stress-strain curves of jammed packings are actually the average of many piecewise linear curves with discontinuous drops in stress, thus the average slope is slightly less than the instantaneous slope [30].

At the unjamming point, the linear response of the system is that of a network of unstretched springs. Thus, at lowest order in pressure the bulk modulus is that of an unstressed spring network, which may be calculated in terms of the “states of self stress,” vectors of possible spring tensions, $s \in \mathbb{R}^Z$, which do not produce any net force on a particle [17, 31, 32]. Here we explain how to carry out this calculation for a monodisperse system in the unjamming limit; a correction for polydispersity is handled in the Supplemental Material.

We begin by defining the set of “affine bond extensions,” a vector $E \in \mathbb{R}^Z$ giving the amount by which each bond vector would increase under a unit volumetric expansion of the system. In linear elasticity, this simply induces an expansion of each length by $1/d$, so,

$$E_\ell = \frac{1}{d} r_\ell, \quad (9)$$

where we emphasize that ℓ indexes the contacts in the system rather than the particles; r_ℓ is the distance between a particular pair of particles.

In the case that all springs have the same spring constant k (e.g., monodisperse packings), the bulk modulus may be written as the projection of these affine moduli onto the states of self stress [17, 31, 32]. At jamming, there is only one state of self stress, and so the bulk modulus may be computed exactly using the projection onto only this one state of self stress [17],

$$K = \frac{k}{V} \left(\sum_{\ell=1}^Z s_{1,\ell} E_\ell \right)^2 \quad (10)$$

In the near jamming limit, this one special state of self stress exists all the way down to the jamming point and can be expressed in terms of the vector of physical force magnitudes, f . For the packing to be in equilibrium, this set of contact forces must produce no net force on every particle, and thus by definition the vector f is always a state of self stress. The projection defined above requires states of self stress to be normalized, and so the state of self stress may be expressed as:

$$s_{1,\ell} = \frac{1}{\sqrt{\sum_i f_i}} f_\ell = \frac{1}{\sqrt{Z \langle f^2 \rangle}} f_\ell. \quad (11)$$

Furthermore at lowest order in P we have $r = \sigma$, and we assume $Z \approx dN$. Thus, Eq. 10 reduces to

$$K = \frac{2Nk\sigma^2 \langle f \rangle^2}{dV \langle f^2 \rangle} = \frac{2N\varepsilon \langle f \rangle^2}{dV \langle f^2 \rangle} \quad (12)$$

and thus via Eq. 8

$$C_{p\varphi} = \frac{2 \langle f \rangle^2}{d \langle f^2 \rangle}, \quad (13)$$

for monodisperse spheres. The full calculation in the Supplemental Material shows that in the polydisperse case this becomes

$$C_{p\varphi} = \frac{2 \langle \sigma f \rangle^2}{d \langle \sigma^2 f^2 \rangle}. \quad (14)$$

We find that the distribution of contact forces does not depend strongly on dimension, which we demonstrate and discuss in the Supplementary Material, including Refs. [28, 33]. We thus predict the scaling of $C_{p\varphi}$ to agree with the asymptotic mean-field scaling. Because this proof does not invoke the mean-field assumption,

we expect this scaling to be correct in all dimensions. Moreover, we are able to calculate each value of $C_{p\varphi}$ by measuring the ratio of force distribution moments. These values are calculated as in Eq. 14, and are shown in Fig. 1 to precisely predict the values of $C_{p\varphi}$.

Conclusion – The mean-field theory of jamming predicts both the scaling exponents and the dimensional scaling of their prefactors. While the exponents have been previously verified, we have demonstrated that even some prefactors are well predicted in low dimensions by mean-field theory. Although these prefactors should be considered especially sensitive to finite dimensional corrections, we find the mean field prediction to be exact in low dimensions. Is this a generic phenomenon, or are the quantities we have chosen to study in this work somehow specially unaffected by finite dimensional correlations? Experience with critical phenomena suggests that although certain ratios of these prefactors (i.e. amplitude ratios) may be universal, the prefactors themselves should be both nonuniversal and challenging to compute, which has led to them being neglected. Our results demonstrate however that these prefactors may be computed exactly. These results call out for other theories of jamming and the glass transition which reproduce the mean-field results without such assumptions, or perhaps for a deeper understanding of why certain mean-field computations may be exact in finite dimensions. Additionally, our results suggest that in traditional critical phenomena mean-field theory may compute more for $d \geq d_u$ than has been previously appreciated.

Acknowledgments – We thank Francesco Zamponi for generous assistance in interpreting the mean-field results. We also thank Andrea Liu, Jim Sethna, Cam Dennis, and Aileen Carroll-Godfrey for valuable discussion and feedback. This work benefited from access to the University of Oregon high performance computer, Talapas. This work was supported by National Science Foundation (NSF) Career Grant No. DMR-1255370 and the Simons Foundation No. 454939 (J.D.S. and E.I.C.) and by an NSERC PGS-D fellowship and Simons Foundation No. 454945 to Andrea J. Liu. (S.A.R.).

-
- [1] Andrea J. Liu and Sidney R. Nagel, “The Jamming Transition and the Marginally Jammed Solid,” *Annual Review of Condensed Matter Physics* **1**, 347–369 (2010).
 - [2] Patrick Charbonneau, Eric I. Corwin, Giorgio Parisi, and Francesco Zamponi, “Universal Microstructure and Mechanical Stability of Jammed Packings,” *Physical Review Letters* **109** (2012), 10.1103/PhysRevLett.109.205501.
 - [3] Patrick Charbonneau, Jorge Kurchan, Giorgio Parisi, Pierfrancesco Urbani, and Francesco Zamponi, “Glass and Jamming Transitions: From Exact Results to Finite-Dimensional Descriptions,” *Annual Review of Condensed Matter Physics* **8**, 265–288 (2017).

- [4] Giorgio Parisi and Francesco Zamponi, “Mean-field theory of hard sphere glasses and jamming,” *Reviews of Modern Physics* **82**, 789–845 (2010).
- [5] Giorgio Parisi, Pierfrancesco Urbani, and Francesco Zamponi, *Theory of Simple Glasses: Exact Solutions in Infinite Dimensions* (Cambridge University Press, New York, 2020).
- [6] Giorgio Parisi, Yoav G. Pollack, Itamar Procaccia, Corrado Rainone, and Murari Singh, “Robustness of mean field theory for hard sphere models,” *Physical Review E* **97** (2018), 10.1103/PhysRevE.97.063003.
- [7] Corey S. O’Hern, Leonardo E. Silbert, Andrea J. Liu, and Sidney R. Nagel, “Jamming at zero temperature and zero applied stress: The epitome of disorder,” *Physical Review E* **68** (2003), 10.1103/PhysRevE.68.011306.
- [8] Corey S. O’Hern, Stephen A. Langer, Andrea J. Liu, and Sidney R. Nagel, “Random Packings of Frictionless Particles,” *Physical Review Letters* **88** (2002), 10.1103/PhysRevLett.88.075507.
- [9] Carl P. Goodrich, Andrea J. Liu, and James P. Sethna, “Scaling ansatz for the jamming transition,” *Proceedings of the National Academy of Sciences* **113**, 9745–9750 (2016).
- [10] Patrick Charbonneau, Eric I. Corwin, Giorgio Parisi, Alexis Poncet, and Francesco Zamponi, “Universal Non-Debye Scaling in the Density of States of Amorphous Solids,” *Physical Review Letters* **117** (2016), 10.1103/PhysRevLett.117.045503.
- [11] Ludovic Berthier, Giulio Biroli, Patrick Charbonneau, Eric I. Corwin, Silvio Franz, and Francesco Zamponi, “Perspective: Gardner Physics in Amorphous Solids and Beyond,” *The Journal of Chemical Physics* **151**, 010901 (2019), arXiv: 1902.10494.
- [12] R. C. Dennis and E. I. Corwin, “Jamming Energy Landscape is Hierarchical and Ultrametric,” *Physical Review Letters* **124** (2020), 10.1103/PhysRevLett.124.078002.
- [13] Francesco Arceri and Eric I. Corwin, “Vibrational properties of hard and soft spheres are unified at jamming,” arXiv:1912.05697 [cond-mat] (2019), arXiv: 1912.05697.
- [14] Carl P. Goodrich, Andrea J. Liu, and Sidney R. Nagel, “Finite-Size Scaling at the Jamming Transition,” *Physical Review Letters* **109** (2012), 10.1103/PhysRevLett.109.095704.
- [15] M. P. Allen, M. P. Allen, D. J. Tildesley, TILDESLEY ALLEN, and D. J. Tildesley, *Computer Simulation of Liquids* (Clarendon Press, 1989).
- [16] Matthieu Wyart, Leonardo E. Silbert, Sidney R. Nagel, and Thomas A. Witten, “Effects of compression on the vibrational modes of marginally jammed solids,” *Physical Review E* **72** (2005), 10.1103/PhysRevE.72.051306.
- [17] M. Wyart, “On the rigidity of amorphous solids,” *Annales de Physique* **30**, 1–96 (2005).
- [18] Alessio Zaccane and Enzo Scossa-Romano, “Approximate analytical description of the nonaffine response of amorphous solids,” *Physical Review B* **83** (2011), 10.1103/PhysRevB.83.184205.
- [19] Danilo B. Liarte, Xiaoming Mao, Olaf Stenull, and T. C. Lubensky, “Jamming as a Multicritical Point,” *Physical Review Letters* **122** (2019), 10.1103/PhysRevLett.122.128006.
- [20] Silvio Franz, Giorgio Parisi, Maxime Sevelev, Pierfrancesco Urbani, and Francesco Zamponi, “Universality of the SAT-UNSAT (jamming) threshold in non-convex continuous constraint satisfaction problems,” *SciPost Physics* **2** (2017), 10.21468/SciPostPhys.2.3.019.
- [21] J A Aronovitz and M J Stephen, “Universal features of the shapes of percolation clusters and lattice animals,” *Journal of Physics A: Mathematical and General* **20**, 2539–2556 (1987).
- [22] V Privman, P. C. Hohenberg, and A Aharony, *Universal Critical-Point Amplitude Relations, in “Phase transition and critical phenomena” vol. 14, C. Domb and JL Lebowitz eds* (Academic Press, 1991).
- [23] E Brizin and J Zinn-Justin, “Finite size effects in phase transitions,” *Nuclear Physics B* **257**, 27 (1985).
- [24] Giorgio Parisi and Juan J. Ruiz-Lorenzo, “Scaling above the upper critical dimension in Ising models,” *Physical Review B* **54**, R3698–R3701 (1996).
- [25] H. W. J Blöte and E Luijten, “Universality and the five-dimensional Ising model,” *Europhysics Letters (EPL)* **38**, 565–570 (1997).
- [26] James D. Sartor and Eric I. Corwin, “Direct measurement of force configurational entropy in jamming,” *Physical Review E* **101** (2020), 10.1103/PhysRevE.101.050902.
- [27] Erik Bitzek, Pekka Koskinen, Franz Gähler, Michael Moseler, and Peter Gumbsch, “Structural Relaxation Made Simple,” *Physical Review Letters* **97** (2006), 10.1103/PhysRevLett.97.170201.
- [28] Patrick Charbonneau, Eric I. Corwin, Giorgio Parisi, and Francesco Zamponi, “Jamming Criticality Revealed by Removing Localized Buckling Excitations,” *Physical Review Letters* **114** (2015), 10.1103/PhysRevLett.114.125504.
- [29] Masanari Shimada, Hideyuki Mizuno, Ludovic Berthier, and Atsushi Ikeda, “Low-frequency vibrations of jammed packings in large spatial dimensions,” arXiv:1910.07238 [cond-mat] (2019), arXiv: 1910.07238.
- [30] Meng Fan, Kai Zhang, Jan Schroers, Mark D. Shattuck, and Corey S. O’Hern, “Particle rearrangement and softening contributions to the nonlinear mechanical response of glasses,” *Physical Review E* **96** (2017), 10.1103/PhysRevE.96.032602.
- [31] S. Pellegrino, “Structural computations with the singular value decomposition of the equilibrium matrix,” *International Journal of Solids and Structures* **30**, 3025–3035 (1993).
- [32] T C Lubensky, C L Kane, Xiaoming Mao, A Souslov, and Kai Sun, “Phonons and elasticity in critically coordinated lattices,” *Reports on Progress in Physics* **78**, 073901 (2015).
- [33] Daniel M. Mueth, Heinrich M. Jaeger, and Sidney R. Nagel, “Force distribution in a granular medium,” *Physical Review E* **57**, 3164–3169 (1998).

Supplementary Material of “Mean-field predictions of scaling prefactors match low-dimensional jammed packings”

James D Sartor*, Sean A. Ridout†, Eric I. Corwin*

**Department of Physics and Materials Science Institute,
University of Oregon, Eugene, Oregon 97403, USA*

†*Department of Physics and Astronomy University of Pennsylvania, Philadelphia, PA 19104, USA*

Measured values of φ_j

In Table I we show our measured values of φ_j . these values are used in calculating $\Delta\varphi$.

Table I: Measured values of φ_j in dimensions 2-10.

d	2	3	4	5	6	7	8	9	10
φ_j	0.85	0.65	0.46	0.31	0.20	0.13	0.078	0.049	0.029

MEAN FIELD PREDICTIONS OF PREFACTORS

Mean Field Prediction of Pressure vs Packing Fraction

Mean field theory predicts that pressure scales with packing fraction as follows [S1]:

$$\hat{P} = \hat{C}(\hat{\varphi} - \hat{\varphi}_j) \quad (S1)$$

where $\hat{C}_{p\varphi}$ is a constant, and the hats over P and $\Delta\varphi$ signify that the quantities are scaled such to be fixed in the infinite dimensional limit, as follows:

$$\hat{P} = \frac{P^*}{\rho d} \quad (S2)$$

$$\hat{\varphi} = \frac{2^d}{d} \varphi \quad (S3)$$

where ρ is the number density, $\frac{N}{V}$, and P^* is the pressure which is calculated with assumed unit particle diameter. This relates to our pressure, P , as follows:

$$P = \frac{\varphi}{\rho} \frac{1}{d^2} P^*, \quad (S4)$$

where the factor of $\frac{\varphi}{\rho}$ unwraps their assumption of unit particle diameter, and the factor of $\frac{1}{d^2}$ comes from their potential, which explicitly contains a dimensional term:

$$U^*(r) = \frac{\epsilon d^2}{2} \left(\frac{r}{\ell} - 1 \right)^2 \Theta(\ell - r). \quad (S5)$$

We can thus rewrite equation S2 in terms of our pressure P :

$$\hat{P} = \frac{d}{\varphi} P, \quad (S6)$$

and therefore equation S1:

$$\frac{d}{\varphi}P = \hat{C} \frac{2^d}{d}(\varphi - \varphi_j) \quad (\text{S7})$$

$$P = \frac{\varphi}{d} \hat{C} \frac{2^d}{d} \Delta\varphi \quad (\text{S8})$$

$$P = \frac{1}{d} \hat{C} \hat{\varphi}_j (\Delta\varphi) \quad (\text{S9})$$

$$P = \frac{1}{d} \hat{C}_{p\varphi} (\Delta\varphi). \quad (\text{S10})$$

Where, noting that $\hat{\varphi}_j$ and \hat{C} are constants in the infinite dimensional limit, we combine them as $\hat{C}_{p\varphi}$. Thus mean field predicts a simple $1/d$ scaling of the prefactor between pressure and excess packing fraction.

Mean Field Prediction of Pressure vs Number Of Excess Contacts

The number of contacts, z , is predicted by mean field theory to have the form [S1]:

$$\frac{z}{2d} = 1 + \hat{C}_{z\varphi} \sqrt{\hat{\varphi} - \hat{\varphi}_j} \quad (\text{S11})$$

$$\frac{z}{2d} = 1 + \hat{C}_{z\varphi} \sqrt{\frac{2^d}{d} \sqrt{\varphi - \varphi_j}} \quad (\text{S12})$$

for some constant $\hat{C}_{z\varphi}$.

The number of excess contacts, δz , therefore is predicted to scale as follows:

$$\frac{\delta z}{2d} = \hat{C}_{z\varphi} \sqrt{\frac{2^d}{d} \sqrt{\varphi - \varphi_j}} \quad (\text{S13})$$

$$\delta z = 2d \hat{C}_{z\varphi} \sqrt{\frac{2^d}{d} \sqrt{\varphi - \varphi_j}}. \quad (\text{S14})$$

Mean Field Prediction of Packing Fraction vs Number of Excess Contacts

By combining equations 10 and 14, we can also predict the relation between δz and P :

$$\delta z = 2d \hat{C}_{z\varphi} \sqrt{\frac{2^d}{d} \sqrt{\frac{d}{\hat{C}_{p\varphi}} P}} \quad (\text{S15})$$

$$= 2d \hat{C}_{z\varphi} \sqrt{\frac{2^d}{\hat{C}_{p\varphi}} \sqrt{P}} \quad (\text{S16})$$

$$(\text{S17})$$

where we define $\hat{C}_{zp} = \frac{2\hat{C}_{z\varphi}}{\sqrt{\hat{C}_{p\varphi}}}$.

Excess Contacts vs Excess Packing Fraction Prefactor Scaling

From eqns 5 and 6 we can simply relate δz and φ as follows:

$$\delta z = C_{z\varphi} (\Delta\varphi)^{1/2} \quad (\text{S18})$$

where clearly,

$$C_{z\varphi} = C_{zp} \sqrt{C_{p\varphi}}. \quad (\text{S19})$$

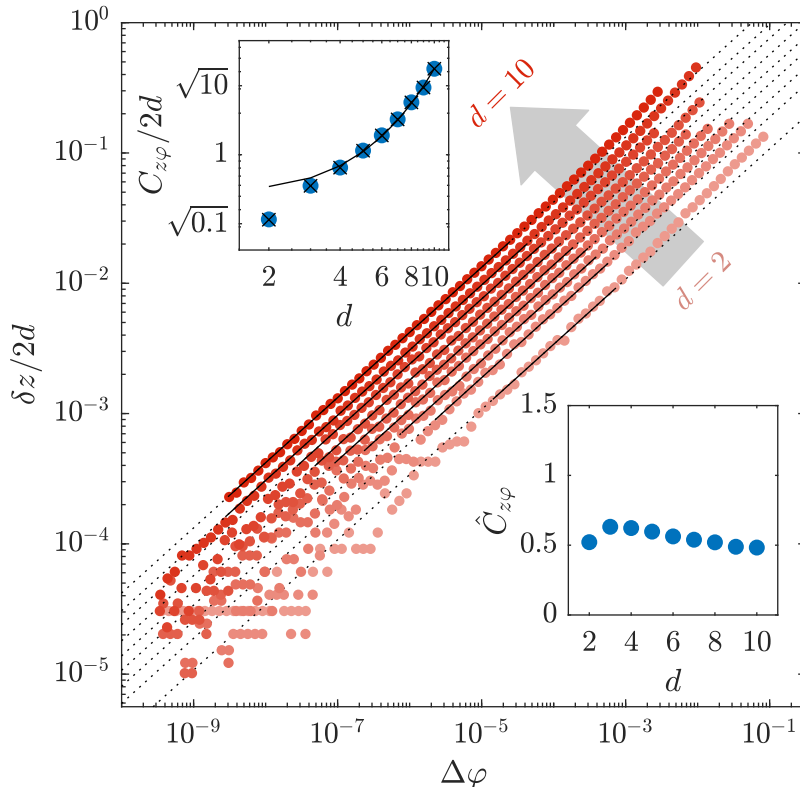


Figure S1: Measured excess contacts scales with the square root of excess packing fraction for systems from $d = 2$ to $d = 10$ (red circles). Black lines show the fits for C_{zp} using eqn S18. For our fits, we ignore data at high pressure and low contact number as in figure 2. Dotted lines show the extension of our fits beyond the fitted range. Inset shows the measured values of $C_{z\varphi}$ (blue circles), which scale in agreement with the mean field prediction eqn S14 using measured values of with $\hat{C}_{z\varphi} \approx 0.83$. Additionally, to note consistency we show that our measured values of $C_{z\varphi}$ agree well with values calculated from our measurements of $C_{p\varphi}$ and C_{zp} using eqn S19 (black x's).

In figure S1, we show this scaling separately for each dimension. We fit each line to eqn S18 to find the values of the prefactor $C_{z\varphi}$ in each dimension, the values of which are shown in the inset. These values agree well with both the mean field prediction above $3D$, shown as a black line, and our calculated value from C_{zp} and $C_{p\varphi}$, shown as black x's in figures 1 and 2.

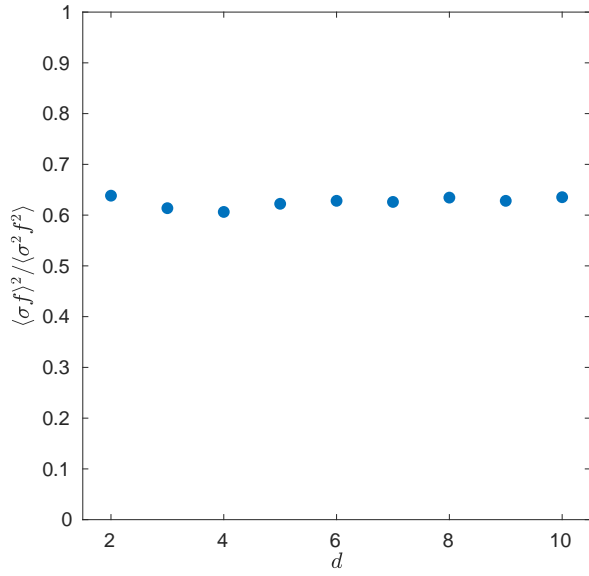
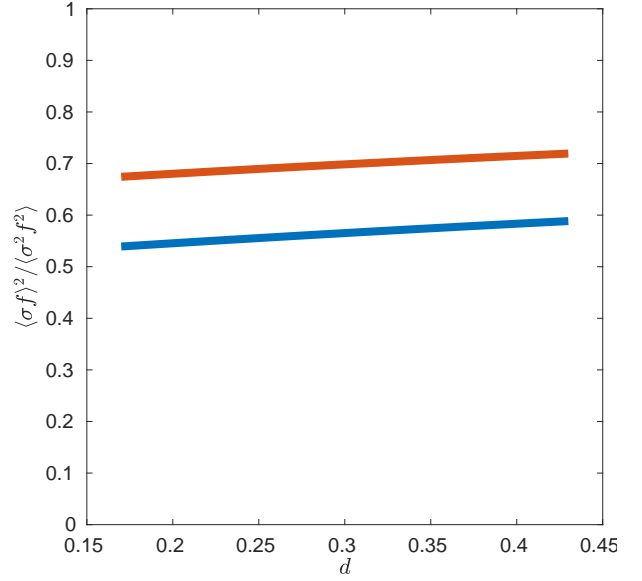
Dimensional Dependence of Force Moment Ratios

In figure S2a we show that the ratio of force moments does not depend strongly on dimension. This empirical fact may seem at odds with previous reports of how the low-force part of the distribution differs from its mean-field form in low dimensions [S2, S3]. The low-force part of the distribution has $P(f) \propto f^\theta$, where $\theta \approx 0.17$ in $d = 2$ smoothly rises to a $d = \infty$ value of $\theta \approx 0.42$. The high-force behaviour decays like an exponential or a stretched exponential; thus, we have computed the theoretical value of this moment ratio for distributions of the form $P(f) \sim f^\theta e^{-f/f_0}$ and $P(f) \sim f^\theta e^{-f^2/f_0^2}$, as shown in figure S2b. We find that neither of these assumed distributions quantitatively predicts the measured moment ratio for the known values of θ , but they do show that the known variation in θ should not make us expect a large variation in this moment ratio.

Accounting for Polydispersity in Pressure vs. Packing Fraction Scaling

To account for the case with varying spring constants we also form the matrix of inverse spring constants

Figure S2: Dimensional dependence of force moment ratios

(a) Dimensionless moment ratio of first and second moments of σf shows no dimensional dependence(b) Neither the force distribution $f^\theta e^{-f/f_0}$ (blue) nor the distribution $f^\theta e^{-f^2/f_0^2}$ (red) predicts a strong θ dependence for the relevant moment ratio

$$k^{-1} = \frac{1}{2\varepsilon} \begin{pmatrix} \sigma_{ij}^2 & & \\ & \ddots & \\ & & \sigma_{kl}^2 \end{pmatrix}. \quad (\text{S20})$$

and the projection operator onto the states of self stress

$$S = \sum_{i=1}^{N\Delta z} |s_i\rangle \langle s_i|. \quad (\text{S21})$$

In terms of these quantities, the bulk modulus may be written as [S4–S6]

$$\frac{\partial^2 E}{\partial V^2} = \frac{1}{V} \langle E | S (S (k^{-1}) S)^{-1} S | E \rangle. \quad (\text{S22})$$

In the one SSS approximation, we can evaluate the two projected quantities that we need to evaluate equation S22. Equations 10 and 12 give

$$S | E \rangle = \langle s_0 | f \rangle | s_0 \rangle = \frac{\langle r | f \rangle}{d \sqrt{\langle f | f \rangle}} | s_0 \rangle = \sqrt{Z} \frac{\langle r f \rangle}{d \sqrt{\langle f^2 \rangle}} | s_0 \rangle, \quad (\text{S23})$$

and equations S20 and 12 give

$$S k^{-1} S = | s_0 \rangle \langle s_0 | k^{-1} | s_0 \rangle \langle s_0 | = | s_0 \rangle \frac{\langle \sigma^2 f^2 \rangle}{2\varepsilon \langle f^2 \rangle} \langle s_0 | \quad (\text{S24})$$

$$(S k^{-1} S)^{-1} = | s_0 \rangle \frac{2\varepsilon \langle f^2 \rangle}{\langle \sigma^2 f^2 \rangle} \langle s_0 | \quad (\text{S25})$$

Furthermore at lowest order in P we have $|r\rangle = |\sigma\rangle$, and we may assume $Z \approx dN$. Thus, equation S22 reduces to

$$K = \frac{2N\varepsilon \langle \sigma f \rangle^2}{dV \langle \sigma^2 f^2 \rangle}, \quad (\text{S26})$$

and thus via equation 9:

$$C_{p\varphi} = \frac{2 \langle \sigma f \rangle^2}{d \langle \sigma^2 f^2 \rangle}. \quad (\text{S27})$$

Prestress Comparison

It has recently been suggested the relationship between prestress and number of excess contacts collapses perfectly when compared across dimensions [S7]. We define prestress e as in ref. [S7] as:

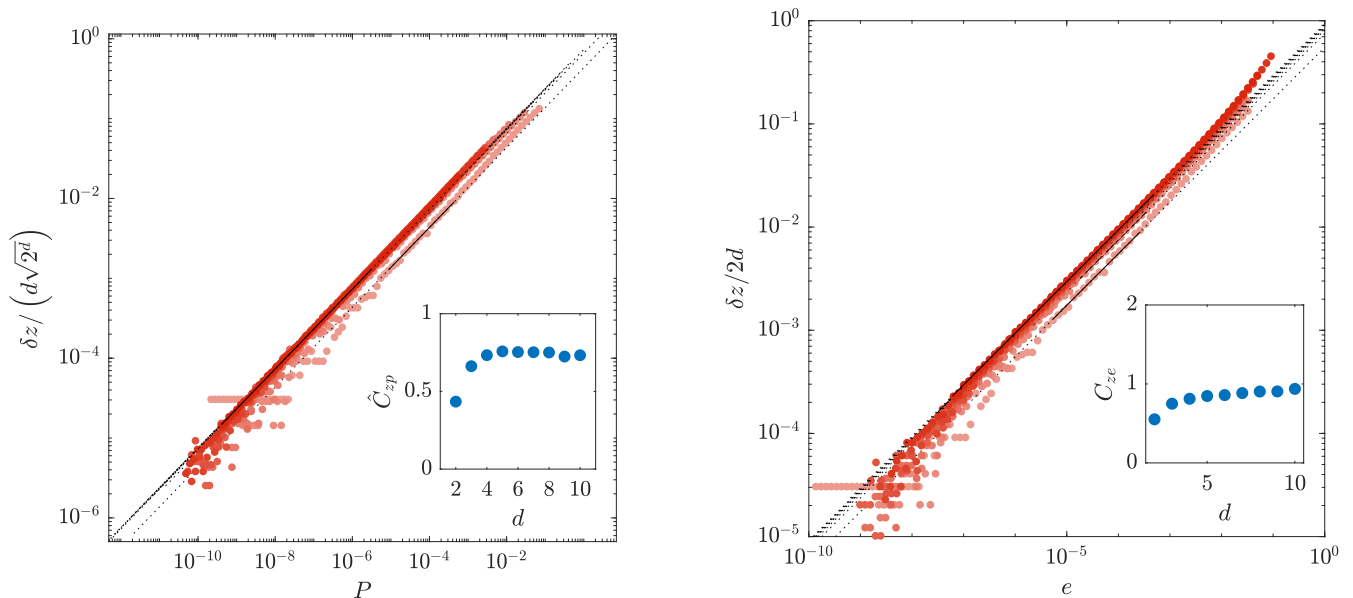
$$e = (d-1) \left\langle \frac{-V'(r_{ij})}{r_{ij} V''(r_{ij})} \right\rangle_{ij} \quad (\text{S28})$$

and expected to scale as:

$$\delta z = C_{ze} e^{\frac{1}{2}} \quad (\text{S29})$$

because it is proportional to pressure near the jamming transition [S7]. In figure S3, we examine the collapse of scaled excess contacts with prestress (fig. S3b), and compare it to the collapse of excess contacts scaled by the mean field prediction with pressure (fig. S3a). In figure S3b we see that the collapse with prestress is not quite perfect - there is a clear upward trend. This stands in contrast to the inset of figure S3a, which shows \hat{C}_{zp} to be nearly constant above three dimensions.

Figure S3: Comparison of scaled excess contacts with pressure and prestress.



(a) Scaled excess contacts scales with the square root of pressure as in figure 2. However, with excess contacts scaled by the expected mean field prediction, eqn. 8, the data collapse onto a single line. The inset confirms the collapse, showing \hat{C}_{zp} to be nearly constant.

(b) Scaled excess contacts scales with the square root of prestress for systems from $d = 2$ to $d = 10$. Black lines show the fits for C_{ze} using eqn S29. The fits ignore high and low pressure data as in figure 2. Lower inset shows the measured values of C_{ze} which have a clear upward trend.

In fact, close to jamming so that $r \approx \sigma$ and $Z \approx Nd$, our dimensionless pressure P as defined in equation 4 is related to the prestress by

$$P = \frac{\bar{V}_p}{\varepsilon V d} \sum_{i,j} \mathbf{f}_{ij} \cdot \mathbf{r}_{ij} \quad (\text{S30})$$

$$= \frac{\bar{V}_p}{\varepsilon V d} Z \langle f_{ij} r_{ij} \rangle_{ij} \quad (\text{S31})$$

$$= \frac{2\varphi Z}{d} \left\langle \frac{r_{ij}}{\sigma_{ij}} \left(1 - \frac{r_{ij}}{\sigma_{ij}} \right) \right\rangle_{ij} \quad (\text{S32})$$

$$= \frac{2\varphi Z}{d} \left\langle \frac{-r_{ij} V'(r_{ij})}{\sigma_{ij}^2 V''(r_{ij})} \right\rangle_{ij} \quad (\text{S33})$$

$$\approx 2 \frac{\varphi_J}{d-1} e. \quad (\text{S34})$$

Thus, our better-fitting form for the $z - P$ relationship amounts to the statement that

$$\frac{\Delta z}{2d} = \hat{C}_\varphi \sqrt{\frac{d}{d-1}} \sqrt{e}. \quad (\text{S35})$$

Thus our scaling forms agree with the statement of reference [S7] in the infinite- d limit, although we see better fit with our form in low dimensions.

-
- [S1] Giorgio Parisi, Pierfrancesco Urbani, and Francesco Zamponi, *Theory of Simple Glasses: Exact Solutions in Infinite Dimensions* (Cambridge University Press, New York, 2020).
- [S2] Patrick Charbonneau, Eric I. Corwin, Giorgio Parisi, and Francesco Zamponi, “Jamming Criticality Revealed by Removing Localized Buckling Excitations,” *Physical Review Letters* **114** (2015), 10.1103/PhysRevLett.114.125504.
- [S3] Daniel M. Mueth, Heinrich M. Jaeger, and Sidney R. Nagel, “Force distribution in a granular medium,” *Physical Review E* **57**, 3164–3169 (1998).
- [S4] S. Pellegrino, “Structural computations with the singular value decomposition of the equilibrium matrix,” *International Journal of Solids and Structures* **30**, 3025–3035 (1993).
- [S5] M. Wyart, “On the rigidity of amorphous solids,” *Annales de Physique* **30**, 1–96 (2005).
- [S6] T C Lubensky, C L Kane, Xiaoming Mao, A Souslov, and Kai Sun, “Phonons and elasticity in critically coordinated lattices,” *Reports on Progress in Physics* **78**, 073901 (2015).
- [S7] Masanari Shimada, Hideyuki Mizuno, Ludovic Berthier, and Atsushi Ikeda, “Low-frequency vibrations of jammed packings in large spatial dimensions,” arXiv:1910.07238 [cond-mat] (2019), arXiv: 1910.07238.